Inversion of qP wave travel times from the URL experiment [1]

Ivan Pšenčík[*], JingSong Liu[**], R. Paul Young[***]

[*] *Geophysical Institute, Acad.Sci.of Czech Republic, Boční II, Praha 4, Czech Republic; e-mail: ip@ig.cas.cz*

[**] *Institute of Geophysics, Chinese Academy of Sciences, P. O. Box 9701, 100101 Beijing, China; e-mail: jsliu@mail.c-geos.ac.cn*

[***] *Dept. of Earth Sciences, The University of Liverpool, 4, Brownlow Street, Liverpool L69 7PG, UK; e-mail: r.p.young@liv.ac.uk*

Abstract

The qP wave travel time data measured during an experiment in the vicinity of the Underground Research Laboratory (URL) in Manitoba, Canada are inverted for elastic parameters. Preliminary results of the inversion are presented. No a priori assumptions about heterogeneity and anisotropy of rocks surrounding the tunnel of the URL is made except the variation of elastic parameters in each grid box, of which the model box is composed, is tri-linear. The qP-wave travel time data from 36 events recorded at 16 receivers yield a very good spatial and angular coverage of the volume, in which the elastic parameters are sought. At the top and in the middle, the resulting model has anisotropy close to orthorhombic symmetry. At the bottom, a different anisotropy can be observed. Maximum velocities at the top and in the middle of the model are slightly deviating from the direction parallel to the axis of the tunnel, with minimum velocities in the direction perpendicular to it. At the bottom, prominent maxima and minima of phase velocities can be found in the plane perpendicular to the axis of the tunnel, along directions deviating about 30^0 from horizontal. The strength of anisotropy decreases slightly with increasing depth. It is shown that a single iteration, from a refernce isotropic medium to an anisotropic medium is insufficient even if the inverted medium is weakly anisotropic. Thus, an iterative inversion procedure must be used. Obtained results indicate that the medium surrounding the tunnel is wekaly anisotropic and that the elastic parameters related to qS-wave propagation cannot be uniquely determined from only qP-wave travel time inversion.

Introduction

In most attempts of tomographic reconstruction in anisotropic media certain limiting assumptions were made in order to reduce the number of parameters to be inverted. Most

[1] Seismic Waves in Complex 3-D Structures, Report 9 (Department of Geophysics, Charles University, Prague 2000), pp.83-112

often the medium is considered to be homogeneous. This is the case of inversions for anisotropy of core samples, see e.g. Jech (1991), Dellinger, Vasicek & Sondergeld (1998). When inhomogeneous media are considered, other simplifications are used. Chapman & Pratt (1992) considered an inhomogeneous medium with general anisotropy but concentrated only on data collected in a 2D plane. Jech & Pšenčík (1992) considered that the medium is inhomogeneous, but of hexagonal symmetry. In both latter cases the authors assumed that the studied anisotropy was weak and thus only a single iteration, from a starting reference isotropic model to a weakly anisotropic resulting model was sufficient. In this contribution, we make no a priori assumptions about inhomogeneity and/or anisotropy of the medium except that a possible variation of elastic parameters within the vicinity of the tunnel is trilinear in each grid box, of which the model box is composed. Since we wish to consider anisotropy of arbitrary strength, we propose an inversion procedure, which is iterative. As in the above mentioned papers, we start from an isotropic medium but then we continue to update obtained anisotropic models in subsequent iterations. Let us mention that such an iterative approach has been used, for example, by Aggio (1994). A substantial difference from Aggio (1994) is that travel times of only qP waves are assumed to be available in this study. This contribution is an extension of the work of Liu & Pšenčík (1999). Instead of synthetic data, experimental data are used this time for tests.

We test the described procedure on a very special set of in-situ observed data, see Maxwell & Young (1995). The data come from an experiment in the Underground Research Laboratory (URL), Manitoba, Canada, performed by Atomic Energy of Canada Limited (AECL) on a site where it studies the implications of disposal of radioactive waste. In the considered experiment, qP wave travel time data generated by 36 sources were collected at 16 receivers surrounding a cylindrical horizontal tunnel known as the Mineby experiment. The sources and receivers were distributed so that a very good spatial and angular coverage of the studied region was reached. We use the above described procedure to invert these data. Maxwell & Young (1995) have inverted the above data assuming hexagonal symmetry of the medium. As stated above we make no assumption about inhomogeneity and type and strength of anisotropy.

In the following, we first present slightly modified formulae used by Liu & Pšenčík (1999). Then we describe , successively, experiments made with the URL data. Analysis of the results is still under way.

Basic formulae

The aim of the inversion is to determine elastic parameters in the considered part of the medium so that they minimize the object function Ω,

$$\Omega = \sum_{i=1}^{N} (\tau_i^{obs} - \tau_i^{cal})^2. \tag{1}$$

Here τ_i^{obs} is the i-th of N observed travel times, τ_i^{cal} is the i-th of N calculated travel times.

As stated above, the procedure is divided into two steps: (a) inversion from an isotropic starting model into an anisotropic model; (b) updating an anisotropic model.

1st step: Inversion from isotropy to anisotropy

The perturbation formula for the qP wave travel times reads

$$\tau = \tau^{iso} - \frac{1}{2}\int_{\tau_0}^{\tau} \alpha^{-2}\Delta a_{ijkl} n_i n_j n_k n_l d\xi = \tau^{iso} - \int_{\tau_0}^{\tau} \frac{\Delta c}{\alpha} d\xi. \tag{2}$$

Here τ^{iso} is the travel time between a source and a receiver in a reference isotropic medium, Δa_{ijkl} is a tensor of deviations of density-normalized elastic parameters from their values in the reference isotropic medium, Δc is a corresponding deviation of the qP wave phase velocity and α is the P wave velocity in the reference isotropic medium. The integration is performed along a ray in the reference medium, n_i being a unit vector tangent to the ray. In an isotropic medium n_i also represents a unit phase normal. According to Pšenčík & Gajewski (1998) the perturbation $\Delta c/\alpha$ can be expressed as

$$\begin{aligned}\frac{\Delta c(n_m)}{\alpha} &= \epsilon_z n_3^4 + 2n_3^3(\epsilon_{34}n_2 + \epsilon_{35}n_1) + n_3^2(\delta_x n_1^2 + \delta_y n_2^2 + 2\chi_z n_1 n_2) \\ &+2n_3(\chi_x n_1^2 n_2 + \chi_y n_1 n_2^2 + \epsilon_{15}n_1^3 + \epsilon_{24}n_2^3) + \epsilon_x n_1^4 + \delta_z n_1^2 n_2^2 \\ &+\epsilon_y n_2^4 + 2\epsilon_{16}n_1^3 n_2 + 2\epsilon_{26}n_1 n_2^3, \end{aligned} \tag{3}$$

where

$$\begin{gathered} \epsilon_x = \frac{A_{11}-\alpha^2}{2\alpha^2}, \quad \epsilon_y = \frac{A_{22}-\alpha^2}{2\alpha^2}, \quad \epsilon_z = \frac{A_{33}-\alpha^2}{2\alpha^2}, \\ \delta_x = \frac{A_{13}+2A_{55}-\alpha^2}{\alpha^2}, \quad \delta_y = \frac{A_{23}+2A_{44}-\alpha^2}{\alpha^2}, \quad \delta_z = \frac{A_{12}+2A_{66}-\alpha^2}{\alpha^2}, \\ \chi_x = \frac{A_{14}+2A_{56}}{\alpha^2}, \quad \chi_y = \frac{A_{25}+2A_{46}}{\alpha^2}, \quad \chi_z = \frac{A_{36}+2A_{45}}{\alpha^2}, \\ \epsilon_{15} = \frac{A_{15}}{\alpha^2}, \quad \epsilon_{16} = \frac{A_{16}}{\alpha^2}, \quad \epsilon_{24} = \frac{A_{24}}{\alpha^2}, \quad \epsilon_{26} = \frac{A_{26}}{\alpha^2}, \quad \epsilon_{34} = \frac{A_{34}}{\alpha^2}, \quad \epsilon_{35} = \frac{A_{35}}{\alpha^2} \end{gathered} \tag{4}$$

are the weak anisotropy (WA) parameters. A great advantage of using the WA parameters is that they are all of the same order, all of them represent a small correction to the parameters specifying the reference isotropic medium. Note that the qP-wave phase velocity is specified by only 15 WA parameters in the approximation (2) and (3).

Let us choose any of the WA parameters and denote it $\epsilon = \epsilon(x, y, z)$. We shall specify the parameter ϵ on a 3D grid by values at grid points. We shall denote by ϵ_{ijk} the value of ϵ at the grid point formed by intersection of x_i, y_j and z_k grid lines, $\epsilon_{ijk} = \epsilon(x_i, y_j, z_k)$. Between grid points, we shall use the three-linear interpolation

$$\epsilon(x,y,z) = \epsilon_{ijk} + A_{100}(x-x_i) + A_{010}(y-y_j) + A_{001}(z-z_k) + A_{110}(x-x_i)(y-y_j)$$

$$+A_{011}(y-y_j)(z-z_k)+A_{110}(x-x_i)(z-z_k)+A_{111}(x-x_i)(y-y_j)(z-z_k). \qquad (5)$$

The coefficients A_{ijk} are defined as follows

$$A_{100}=\frac{\epsilon_{i+1jk}-\epsilon_{ijk}}{x_{i+1}-x_i}, \quad A_{010}=\frac{\epsilon_{ij+1k}-\epsilon_{ijk}}{y_{j+1}-y_j}, \quad A_{001}=\frac{\epsilon_{ijk+1}-\epsilon_{ijk}}{z_{k+1}-z_k},$$

$$A_{110}=\frac{\epsilon_{i+1j+1k}-\epsilon_{i+1jk}-\epsilon_{ij+1k}+\epsilon_{ijk}}{(x_{i+1}-x_i)(y_{j+1}-y_j)}, \quad A_{011}=\frac{\epsilon_{ij+1k+1}-\epsilon_{ij+1k}-\epsilon_{ijk+1}+\epsilon_{ijk}}{(y_{j+1}-y_j)(z_{k+1}-z_k)},$$

$$A_{101}=\frac{\epsilon_{i+1jk+1}-\epsilon_{i+1jk}-\epsilon_{ijk+1}+\epsilon_{ijk}}{(x_{i+1}-x_i)(z_{k+1}-z_k)},$$

$$A_{111}=\frac{\epsilon_{i+1j+1k+1}-\epsilon_{i+1j+1k}-\epsilon_{ij+1k+1}-\epsilon_{i+1jk+1}+\epsilon_{i+1jk}+\epsilon_{ij+1k}+\epsilon_{ijk+1}-\epsilon_{ijk}}{(x_{i+1}-x_i)(y_{j+1}-y_j)(z_{k+1}-z_k)}. \qquad (6)$$

In order to minimize (1), we need to know the derivatives $\partial\tau/\partial\epsilon_{ijk}$ of travel times with respect to ϵ_{ijk}. Differentiating Eq.(2), we get

$$\frac{\partial\tau}{\partial\epsilon_{ijk}}=-\int_{\tau_0}^{\tau}\alpha^{-1}\frac{\partial\Delta c}{\partial\epsilon}\frac{\partial\epsilon}{\partial\epsilon_{ijk}}d\xi. \qquad (7)$$

The derivative $\partial\Delta c/\partial\epsilon$ can be obtained by differentiating Eq.(3) with respect to the corresponding WA parameter. This yields

$$\frac{\partial\Delta c}{\partial\epsilon_x}=\alpha n_1^4, \quad \frac{\partial\Delta c}{\partial\epsilon_y}=\alpha n_2^4, \quad \frac{\partial\Delta c}{\partial\epsilon_z}=\alpha n_3^4,$$

$$\frac{\partial\Delta c}{\partial\delta_x}=\alpha n_1^2n_3^2, \quad \frac{\partial\Delta c}{\partial\delta_y}=\alpha n_2^2n_3^2, \quad \frac{\partial\Delta c}{\partial\delta_z}=\alpha n_1^2n_2^2,$$

$$\frac{\partial\Delta c}{\partial\chi_z}=2\alpha n_1n_2n_3^2, \quad \frac{\partial\Delta c}{\partial\chi_x}=2\alpha n_1^2n_2n_3, \quad \frac{\partial\Delta c}{\partial\chi_y}=2\alpha n_1n_2^2n_3,$$

$$\frac{\partial\Delta c}{\partial\epsilon_{15}}=2\alpha n_1^3n_3, \quad \frac{\partial\Delta c}{\partial\epsilon_{16}}=2\alpha n_1^3n_2, \quad \frac{\partial\Delta c}{\partial\epsilon_{24}}=2\alpha n_2^3n_3,$$

$$\frac{\partial\Delta c}{\partial\epsilon_{26}}=2\alpha n_1n_2^3, \quad \frac{\partial\Delta c}{\partial\epsilon_{34}}=2\alpha n_2n_3^3, \quad \frac{\partial\Delta c}{\partial\epsilon_{35}}=2\alpha n_1n_3^3. \qquad (8)$$

The derivatives $\partial\epsilon/\partial\epsilon_{ijk}$ can be obtained by differentiating $\epsilon(x,y,z)$ in Eq.(5) with respect to ϵ_{ijk}. This yields

$$\frac{\partial\epsilon}{\partial\epsilon_{ijk}}=1-\frac{x-x_i}{x_{i+1}-x_i}-\frac{y-y_j}{y_{j+1}-y_j}-\frac{z-z_k}{z_{k+1}-x_k}+\frac{(x-x_i)(y-y_j)}{(x_{i+1}-x_i)(y_{j+1}-y_j)}$$

$$+\frac{(y-y_j)(z-z_k)}{(y_{j+1}-y_j)(z_{k+1}-z_k)}+\frac{(x-x_i)(z-z_k)}{(x_{i+1}-x_i)(z_{k+1}-z_k)}-\frac{(x-x_i)(y-y_j)(z-x_k)}{(x_{i+1}-x_i)(y_{j+1}-y_j)(z_{k+1}-z_k)},$$

$$\frac{\partial\epsilon}{\partial\epsilon_{i+1jk}}=\frac{x-x_i}{x_{i+1}-x_i}-\frac{(x-x_i)(y-y_j)}{(x_{i+1}-x_i)(y_{j+1}-y_j)}$$

$$-\frac{(x-x_i)(z-z_k)}{(x_{i+1}-x_i)(z_{k+1}-z_k)}+\frac{(x-x_i)(y-y_j)(z-x_k)}{(x_{i+1}-x_i)(y_{j+1}-y_j)(z_{k+1}-z_k)}, \tag{9}$$

etc.

2nd step: Inversion from anisotropy to anisotropy

In the first step of the inversion we found only 15 qP-wave WA parameters, from which we can uniquely determine only 9 elastic parameters, see Eq.(4). For tracing rays in an inhomogeneous generally anisotropic medium, we need, however, to know either all 21 WA parameters or all 21 elastic parameters. In order to determine the remaining 6 WA parameters related to qS waves,

$$\gamma_x=\frac{A_{55}-\beta^2}{2\beta^2},\quad \gamma_y=\frac{A_{44}-\beta^2}{2\beta^2},\quad \gamma_z=\frac{A_{66}-\beta^2}{2\beta^2},\quad \epsilon_{46}=\frac{A_{46}}{\beta^2},\quad \epsilon_{56}=\frac{A_{56}}{\beta^2},\quad \epsilon_{45}=\frac{A_{45}}{\beta^2} \tag{10}$$

we must make assumptions about their values. A possible assumption is

$$\gamma_x=\epsilon_x,\qquad \gamma_y=\epsilon_y,\qquad \gamma_z=\epsilon_z,\qquad \epsilon_{46}=\epsilon_{56}=\epsilon_{45}=0. \tag{11a}$$

This implies

$$A_{44}=\frac{\beta^2}{\alpha^2}A_{22},\qquad A_{55}=\frac{\beta^2}{\alpha^2}A_{11},\qquad A_{66}=\frac{\beta^2}{\alpha^2}A_{33},\qquad A_{46}=A_{56}=A_{45}=0. \tag{11b}$$

Remaining 6 elastic parameters can be now easily determined from Eqs.(4). In this way, we can construct complete stiffness matrix, which serves as an initial guess for the second step of inversion procedure. All 21 elastic parameters can be sought in the second and higher iterations.

The perturbation formula for travel time when the reference medium is anisotropic reads, see Jech & Pšenčík (1989)

$$\tau=\tau^{ani}-\frac{1}{2}\int_{\tau_0}^{\tau}\Delta a_{ijkl}p_i g_j g_k p_l d\xi=\tau^{ani}-\frac{1}{2}\int_{\tau_0}^{\tau}\Delta G d\xi, \tag{12}$$

Here τ^{ani} is the travel time between a source and a receiver in a reference anisotropic medium determined during the previous iteration, p_i denote components of the slowness vector and g_i components of the unit polarization vector, both calculated along the ray in the reference medium. The values p_i and g_i are automatically generated when a ray is calculated in an anisotropic medium by the program ANRAY (Gajewski & Pšenčík (1990).

The derivatives necessary for inversion, $\partial\Delta\tau/\partial A_{\alpha\beta,ijk}$, where $A_{\alpha\beta,ijk}$ is the value of the parameter $A_{\alpha\beta}$ at the grid point (x_i, y_j, z_k) and $\alpha,\ \beta = 1, 2, .., 6$, read

$$\frac{\partial\tau}{\partial A_{\alpha\beta,ijk}} = -\frac{1}{2}\int_{\tau_0}^{\tau} \frac{\partial\Delta G}{\partial A_{\alpha\beta}} \frac{\partial A_{\alpha\beta}}{\partial A_{\alpha\beta,ijk}} d\xi. \tag{13}$$

The derivative $\partial\Delta G/\partial A_{\alpha\beta}$ can be obtained by taking into account the definition of ΔG in (9). We get

$$\frac{\partial\Delta G}{\partial A_{11}} = p_1^2 g_1^2, \quad \frac{\partial\Delta G}{\partial A_{22}} = p_2^2 g_2^2, \quad \frac{\partial\Delta G}{\partial A_{33}} = p_3^2 g_3^2,$$

$$\frac{\partial\Delta G}{\partial A_{12}} = 2p_1p_2g_1g_2, \quad \frac{\partial\Delta G}{\partial A_{13}} = 2p_1p_3g_1g_3, \quad \frac{\partial\Delta G}{\partial A_{23}} = 2p_2p_3g_2g_3,$$

$$\frac{\partial\Delta G}{\partial A_{14}} = 2p_1g_1g_2p_3 + 2p_1g_1g_3p_2, \qquad \frac{\partial\Delta G}{\partial A_{15}} = 2p_1g_1g_1p_3 + 2p_1g_1g_3p_1,$$

$$\frac{\partial\Delta G}{\partial A_{16}} = 2p_1g_1g_1p_2 + 2p_1g_1g_2p_1, \qquad \frac{\partial\Delta G}{\partial A_{24}} = 2p_2g_2g_2p_3 + 2p_2g_2g_3p_2,$$

$$\frac{\partial\Delta G}{\partial A_{25}} = 2p_2g_2g_1p_3 + 2p_2g_2g_3p_1, \qquad \frac{\partial\Delta G}{\partial A_{26}} = 2p_2g_2g_1p_2 + 2p_2g_2g_2p_1,$$

$$\frac{\partial\Delta G}{\partial A_{34}} = 2p_3g_3g_2p_3 + 2p_3g_3g_3p_2, \qquad \frac{\partial\Delta G}{\partial A_{35}} = 2p_3g_3g_1p_3 + 2p_3g_3g_3p_1,$$

$$\frac{\partial\Delta G}{\partial A_{36}} = 2p_3g_3g_1p_2 + 2p_3g_3g_2p_1, \qquad \frac{\partial\Delta G}{\partial A_{44}} = 2p_2g_3g_2p_3 + p_2^2g_3^2 + p_3^2g_2^2,$$

$$\frac{\partial\Delta G}{\partial A_{55}} = 2p_1g_3g_1p_3 + p_1^2g_3^2 + p_3^2g_1^2, \qquad \frac{\partial\Delta G}{\partial A_{66}} = 2p_1g_2g_1p_2 + p_1^2g_2^2 + p_2^2g_1^2,$$

$$\frac{\partial\Delta G}{\partial A_{45}} = 2p_2g_3g_1p_3 + 2p_3g_2g_1p_3 + 2p_2g_3g_3p_1 + 2p_3g_2g_3p_1,$$

$$\frac{\partial\Delta G}{\partial A_{46}} = 2p_2g_3g_1p_2 + 2p_3g_2g_1p_2 + 2p_2g_3g_2p_1 + 2p_3g_2g_2p_1,$$

$$\frac{\partial\Delta G}{\partial A_{56}} = 2p_1g_3g_1p_2 + 2p_3g_1g_1p_2 + 2p_1g_3g_2p_1 + 2p_3g_1g_2p_1. \tag{14}$$

The derivatives $\partial A_{\alpha\beta}/\partial A_{\alpha\beta,ijk}$ can be obtained from Eq.(9) if we substitute ϵ by $A_{\alpha\beta}$ and ϵ_{ijk} by $A_{\alpha\beta,ijk}$.

Inversion of the URL data in geographic coordinates

We consider the data set and the configuration described by Maxwell & Young (1995); for the configuration, see their Figure 1. We consider a Cartesian coordinate system whose positive x-coordinate points to north, positive y-coordinate points to east and positive z-coordinate points downwards. We concentrate on a model box specified as follows: x is in the interval $< 412, 460 >$, y in $< 735, 782 >$ and z in $< 109, 145 >$. All values are in metres. The tunnel is practically a cylindrical horizontal body with the radius of 1.75 m, oriented in the southwest direction, i.e. 45^o from north. The axis of the tunnel intersects its face at the point with coordinates [453.07, 775.50, 125.76] in meters. The model box consists of a single grid box. Thus the corners of the model box are points, in which we seek the values of elastic parameters ϵ_{ijk}. Inside the box a tri-linear interpolation (5) is considered. No additional assumption about inhomogeneity and/or anisotropy of the model is made. Thus, 15 WA parameters are sought in the first step of the inversion and all 21 elastic parameters are sought at each of the 8 corners of the model box in subsequent iterations. The starting reference model is homogeneous and isotropic. For all the higher iterations, the refernce model is generally inhomogeneous and anisotropic. The SVD technique is used for solving the system of linear equations resulting from the condition of minimization of the object function (1). Synthetic travel times between sources and receivers in an inhomogeneous isotropic and anisotropic media are calculated by a modified version of the ANRAY program package, see Gajewski & Pšenčík (1990).

As sources, explosions fired from 36 short (40-70cm length) boreholes along the length of the tunnel were used. Survey was performed using 16 sensors. For the inversion, only travel times corresponding to source-receiver pairs whose straight line connections did not intersect or touch the tunnel were considered. This requirement reduced the number of travel times to 415. Since the number of sought parameters is 8x21, i.e., 168, the inverse problem is sufficiently overdetermined. In the present experiment the travel time data were inverted without taking into account any error in their picking. Projections of the straight line connections of all considered source-receiver pairs are shown in Figure 1. Figure 1a shows the projections into a horizontal (x, y) plane, Figure 1b shows the projections into the vertical planes (y, z) and (x, z). Red open circles denote positions of sources.

Apparent velocities versus azimuths for source-receiver straight lines within 20^o of the (y, z) plane (top), (x, z) plane (middle) and (x, y) plane (bottom) are shown in Figure 2. The bottom picture corresponds to open circle data in Figure 3 of Maxwell & Young (1995). We can see that angular dependence of apparent velocities is most pronounced in the horizontal plane but certain variations can also be observed in both vertical planes.

Since an average apparent velocity in Figure 2 seems to be approximately 5.7 km/s, we choose the squares of P and S wave velocities in the reference homogeneous isotropic model to be 33 and 11 $(\mathrm{km/s})^2$ respectively. After approximately 7 iterations the results of inversion stabilized as can be seen from Figure 3. Figure 3 shows the variation of the root mean square misfit of observed and synthetic travel times with increasing number of iterations. The convergency is considerably faster than in the inversion of synthetic VSP data set, see Liu & Pšenčík (1999). The obvious reason is an excellent angular coverage of the studied region in the URL experiment.

The most dramatic change always occured during the first step, i.e., during the iteration from the homogeneous isotropic reference medium to the inhomogeneous anisotropic medium. This can be seen in Figures 4-6, which show sections of phase velocities calculated during several initial iterations. The matrices of elastic parameters at the top and the bottom of the model box, used for the generation of Figures 4-6, were obtained by averaging the values obtained at the four top and the four bottom corners of the model box. Figure 4 shows (x, z) sections at the top of the model box (top) and at its bottom (bottom). The horizontal black line corresponds to the isotropic reference medium (P wave velocity of approximately 5.75 km/s). The red line shows the results of the first iteration, the green line results of the 7th iteration. Figure 5 shows (y, z) sections and Figure 6 (x, y) sections. We can see that even iterations higher than one lead to significant changes in behaviour of phase velocities. Using only the first iteration, as Jech & Pšenčík (1992) did, would lead to incomplete results.

The results presented in Figures 4-6 were obtained with the starting reference isotropic model specified by $\alpha^2 = 33$ (km/s)^2. It is of interest to see how the results of inversion depend on the choice of the starting isotropic model. For this purpose we inverted the travel time data with two additional isotropic refernce media. In the first $\alpha^2 = 36$ and $\beta^2 = 12$ (km/s)^2, in the second $\alpha^2 = 25$ and $\beta^2 = 8.33$ (km/s)^2. If we compare corresponding P wave velocities with the apparent velocities shown in Figure 2, we can see that the velocity of the first reference medium corresponds approximately to the upper limit of the observed apparent velocities, the velocity of the second reference medium is significantly below the lower limit. In Figures 7-9, we show comparison of final results (corresponding to 7th iteration) corresponding to different reference isotropic models in the same form as we showed individual iterations in Figures 4-6. The black curve corresponds to the isotropic reference medium with $\alpha^2 = 25$ (km/s)^2, red curve shows the results for the reference medium with $\alpha^2 = 33$ (km/s)^2, i.e. it shows the results of final iteration from Figures 4-6, and the green curve shows the results for the reference medium with $\alpha^2 = 36$ (km/s)^2. Results shown by the red and green curves are quite similar, the results shown by the black curve differ. They not only differ by a different angular dependence, mostly in the deeper parts of the model, but also by a rather strong, probably unrealistic vertical gradient. It is also interesting that the phase velocity for the reference medium of 5 km/s, reaches maximum velocity of all the considered refernce media in the bottom part of the final model. All this indicates that the model shown by the black curve should not be considered too seriously. Since the difference of the remaining two curves is small (the maximum deviation of the red and green curves is below 2%), we conclude that they map regions of acceptable solutions.

For making conclusions concerning the overall angular behaviour of phase velocities, the above sections are insufficient. In Figure 10 we show, therefore, continuous angular distribution of phase velocities obtained with the isotropic reference medium $\alpha^2 = 33$ (km/s)^2. Fig.10a (10b) shows the phase velocities at the corner points of the upper (lower) horizontal boundary of the model. The frames u01, u02, u03 and u04 (l01, l02, l03 and l04) correspond, successively, to the lower left, lower right, upper left and upper right corner points in Fig.1a. The qP-wave phase velocity values are shown in a plot covering azimuthal and polar angles between 0^o and 180^o, i.e., over a half sphere. The vertical line with the azimuth of 0^o corresponds to the (x, z) section shown by red line in Figure 5, the vertical line with the azimuth of 90^o corresponds to the (y, z) section shown in Figure 6. Polar angle 0^o corresponds to a horizontal direction, 90^o to vertical direction. The phase velocities are shown by isolines on the gray scaled background. The gray scale is used to indicate the variation of phase velocities between isolines.

From Figure 10a we can see that there are, very roughly, one velocity maximum at azimuth of about 40^o in a direction declining by about 30^o from horizontal and two minima, one in the vertical direction and the other one at azimuth of about 130^o in a horizontal direction. The maximum velocity is about 6.0 km/s, the minimum velocity about 5.40 km/s. Such a configuration of maxima and minima resembles an orthorhombic symmetry. It is worth recalling that the axis of the tunnel is horizontal, its azimuth being 45^o degrees. Thus the maximum velocity in Figure 10a points approximately (if we neglect the declination) along the axis of the tunnel and the minima of velocity are in directions close to perpendicular to the axis of the tunnel. Figure 10b differs from Figure 10a by two features. First, the distribution of maxima and minima in the plots does not have such a regular character as in Fig.10a. The maxima are shallower than in Fig.10a, and, except the plot l02, they are shifted to greater azimuths while "horizontal" minima remain at nearly the same azimuths as in Fig.10a. Second, while the maximum velocities in Figs.10a and 10b are nearly the same, the minimum velocities in Fig.10b are higher, about 5.63 km/s. Anisotropy at the bottom of the model is thus slightly weaker than at its top. This could already be observed from Figures 4-9.

The above results indicate that the orientation of the tunnel obviously controls the symmetry of the surrounding medium. They also indicate that the properties of the medium are different at the top and the bottom of the model box containing the tunnel. We decided, therefore, to make the following experiments. First, we decided to substitute the geographic coordinate system used in the previous inversion by a more natural "tunnel" coordinate system with x-axis coinciding with axis of the tunnel. Second, we decided to study consequences of allowing more general variation of parameters in the model than the trilinear interpolation within a single grid box used in the previous inversion.

Inversion of the URL data in "tunnel" coordinates

We chose the origin of the "tunnel" coordinate system at the point with coordinates [436.0, 760., 125.76]. At this point we rotated the "URL" coordinate system around the z-axis by 45^0 so that the x-axis of the new coordinate system coincided with the axis of the tunnel. In the new coordinate system we specified the model box as follows: x is in the interval $< -24, 24 >$, y in $< -25, 22 >$ and z in $< 109, 145 >$. All values are in metres.

Apparent velocities versus azimuths for source-receiver straight lines within 20^o of the (y, z) plane (top), (x, z) plane (middle) and (x, y) plane (bottom) in the new coordinate system are shown in Figure 11. From comparison of Fig.11 with Fig.2 we can see clear axial symmetry pattern in Fig.11 connected with the choice of the "tunnel" coordinate system.

The results of inversion in the new coordinate system are shown in Fig.12. The arrangement of plots is the same as in Figs.10a and 10b. In Fig.12a, which shows the top of the model, we can see that maxima of phase velocities are shifted towards the corners of diagrams, which correspond to the axis of the tunnel. Minima are situated close to directions perpendicular to the tunnel. The plots resemble again the orthorhombic symmetry. The plots in Fig.12b, corresponding to the bottom of the model are more complicated. Instead of a single maximum, two maxima of nearly the same strength appear in this case. The maxima do not point in the direction of the axis of the tunnel. We can also observe a difference in behaviour of phase velocities at the front part (l01, l03) of the tunnel and its rear part (l02, l04).

We wanted to see if the described pattern is not a consequence of a limited freedom of variation of parameters of the medium in the model box. The above results were obtained with the model box consisting of a single the grid box, within which trilinear interpolation (5) was used. This means that we sought elastic parameters at 8 corner points of the model box. We decided to repeat the inversion with the model box consisting of 4 grid boxes with common edge formed by the axis of the tunnel. In this way, we sought elastic parameters at 18 corner points. The results are shown in Figure 13. The arrangement of individual plots is slightly different from Figs.10 and 12. Figure 13a shows the situation in the front part of the tunnel, Fig.13b in the rear. The upper plots correspond to the top of the model, the middle plots to its middle and the bottom plots to the bottom of the model. The marked frames correspond to the frames with the same mark in Figs.12a and 12b.

Figure 13 confirms a distinct difference between the top (and now even the middle) of the model and the bottom. It seems that the change is caused more by change of anisotropy than of its strength. Maximum velocities at all levels are close to 6.0 km/s, minimum velocities are are about 5.5 km/s at the top and the middle and about 5.65 km/s at the bottom. The maximum velocity declines by about 20^o from the axis of the tunnel. Generally, the results shown in Fig.13 seem to confirm observations made in Fig.12.

Effects of the choice of the qS-wave WA parameters

It is necessary to clear out the role of the choice of the WA parameters related to qS waves, see Eqs.(11). This is shown in Fig.14. The upper left plot corresponds to data obtained during the inversion and was obtained from exact formula specified by all 21 elastic parameters. In the upper right and bottom left plots we show how the phase velocity depends on WA parameters, in this case on δ_z specifically. As it can be seen from Eq.(4), the WA parameter δ_z contains the combination $A_{12} + 2A_{66}$ of elastic parameters. The bottom left plot shows that any change of A_{12} and A_{66}, which preserves δ_z, has no or negligible effect on the phase velocity. Only a change which leads to a change of δ_z leads to a change of the phase velocity, as can bee seen on the upper right plot. This means that the choice (11) of the remaining WA parameters has practically no effect on inverted qP-wave phase velocities. This was also confirmed by numerical tests.

The bottom right plot was obtained from the qP-wave WA formula (which can be obtained from Eq.(3) by adding to it the reference P-wave velocity), which is specified by only 15 qP-wave WA parameters. An excellent fit of this plot with the upper left plot obtained from the exact formula indicates that the studied medium can be considered as weakly anisotropic, and that there is no chance to determine the WA parameters related to qS-waves from the qP-wave travel time data alone.

Conclusion and discussion

Conclusions can be divided into two parts: conclusions concerning the proposed procedure and conclusions concerning the obtained results.

Inversion for all 21 elastic parameters from qP wave travel time observations only, starting from a homogeneous isotropic model proved to be feasible. Inversion consists of two separate steps. First step from isotropy to anisotropy yields only 15 WA parameters, see Eq.(4). All 21 elastic parameters are obtained in subsequent iterations from anisotropic starting model to an updated anisotropic model when 6 remaining WA parameters are determined artificially. It turned out that although the first step yielded results whose basic features remained preserved during subsequent iterations, results of the first iteration still differ significantly from the final results. This implies that higher iterations should be used generally, even in weakly anisotropic media. The experiment with varying reference isotropic medium seems to show that acceptable results of inversion depend only slightly on the choice of the starting reference isotropic model (if it does not deviate considerably from what is indicated by data). It was also shown that, at least in the studied case, the inversion is not affected by the artificial choice of the WA parameters related to qS-waves. In fact, in the considered experiment these parameters cannot be determined from the qP-wave travel time data alone.

Comparison of obtained results with results of Maxwell and Young (1995) shows several interesting differencies. First, it seems that the medium is not hexagonally symmetric as assumed by the above authors but it has lower symmetry, at the top and the middle of the model resembling orthorhombic symmetry. The results of our inversion show a vertical variation of anisotropy combined with a slight decrease in its strength. The lower strength of anisotropy at the floor could be probably associated with more confinement due to waste on the floor of the tunnel closing some microcracks and or greater saturation due to water on the floor of the tunnel. In the roof region loose material falls out and desaturation in the damage zone in the immediate vicinity of the tunnel takes place. In the immediate excavation damage zone the cracks are predominantly tangential. However, the microcracks caused by the far field stresses are expected to be orthogonal to the tunnel axis. Combination of these two systems of parallel cracks might be the reason for the observed symmetry, which is close to orthorhombic symmetry.

Both the procedure and the results of the inversion of the URL data require further intensive analysis and tests.

Acknowledgement

This work was supported by the consortium project "Seismic waves in complex 3-D structures (SW3D)". The first named author appreciates support of the Grant Agency of the Czech Republic under the contract 205/00/1350. The figures were plotted with the SU software of CWP, Colorado School of Mines.

References

Aggio,A.S., 1995. Inversion of qS and qP waves from VSP data in 3D heterogeneous anisotropic media with hexagonal or orthorhombic symmetry. PhD thesis, UFBa Salvador, Brazil (in Portuguese).

Carlson, S. R. & Young, R.P., 1993. Acoustic emission and ultrasonic velocity study of excavation-induced microcrack damage in the Mine-By tunnel wall at the Underground Research Laboratory, Pinawa, Manitoba. *Int. J. of Rock Mechanics and Mining Sci.*, **30**, 901-909.

Chapman,C.H. & Pratt,R.G., 1992. Traveltime tomography in anisotropic media-I. Theory: *Geophys.J.Int.*, **109**, 1-19.

Dellinger.L., Vasicek,D. & Sondergeld,C., 1998. Kelvin notation for stabilizing elastic-constant inversion. *Revue de l'Inst.Franc.du Pétrole*, **53**, 709-719.

Falls, S.D. & Young, R.P., 1998. Acoustic emission and ultrasonic-velocity methods used to characterise the excavation disturbance associated with deep tunnels in hard rock. *Tectonophysics*, **289**, 1-15.

Gajewski,D. & Pšenčík,I., 1990. Vertical seismic profile synthetics by dynamic ray tracing in laterally varying layered anisotropic structures. *J.geophys.Res.*, **95**, 11301-11315.

Jech,J., 1991. Computation of elastic parameters of anisotropic medium from travel times of quasi-compressional waves. *Phys. Earth Planet. Inter.*, **66**, 153-159.

Jech,J. & Pšenčík,I., 1989. First-order perturbation method for anisotropic media. *Geophys.J.Int.*, **99**, 369-376.

Jech,J. & Pšenčík,I., 1992. Kinematic inversion for qP and qS waves in inhomogeneous anisotropic structures. *Geophys.J.Int.*, **108**, 604-612.

Liu,J. & Pšenčík,I., 1999. Inversion of qP wave travel times: Synthetic study. In: Seismic Waves in Complex 3-D Structures, Report 8, pp.27-46, Dept.of Geophysics, Charles University Prague.

Maxwell,S.C. & Young,R.P., 1995. A controlled in-situ investigation of the relationship between stress, velocity and induced seismicity. Geophys. Res. Letters., **22**, 1049-1052.

Pšenčík,I. & Gajewski,D., 1998. Polarization, phase velocity and NMO velocity of qP waves in arbitrary weakly anisotropic media. *Geophysics*, **63**, 1754-1766.

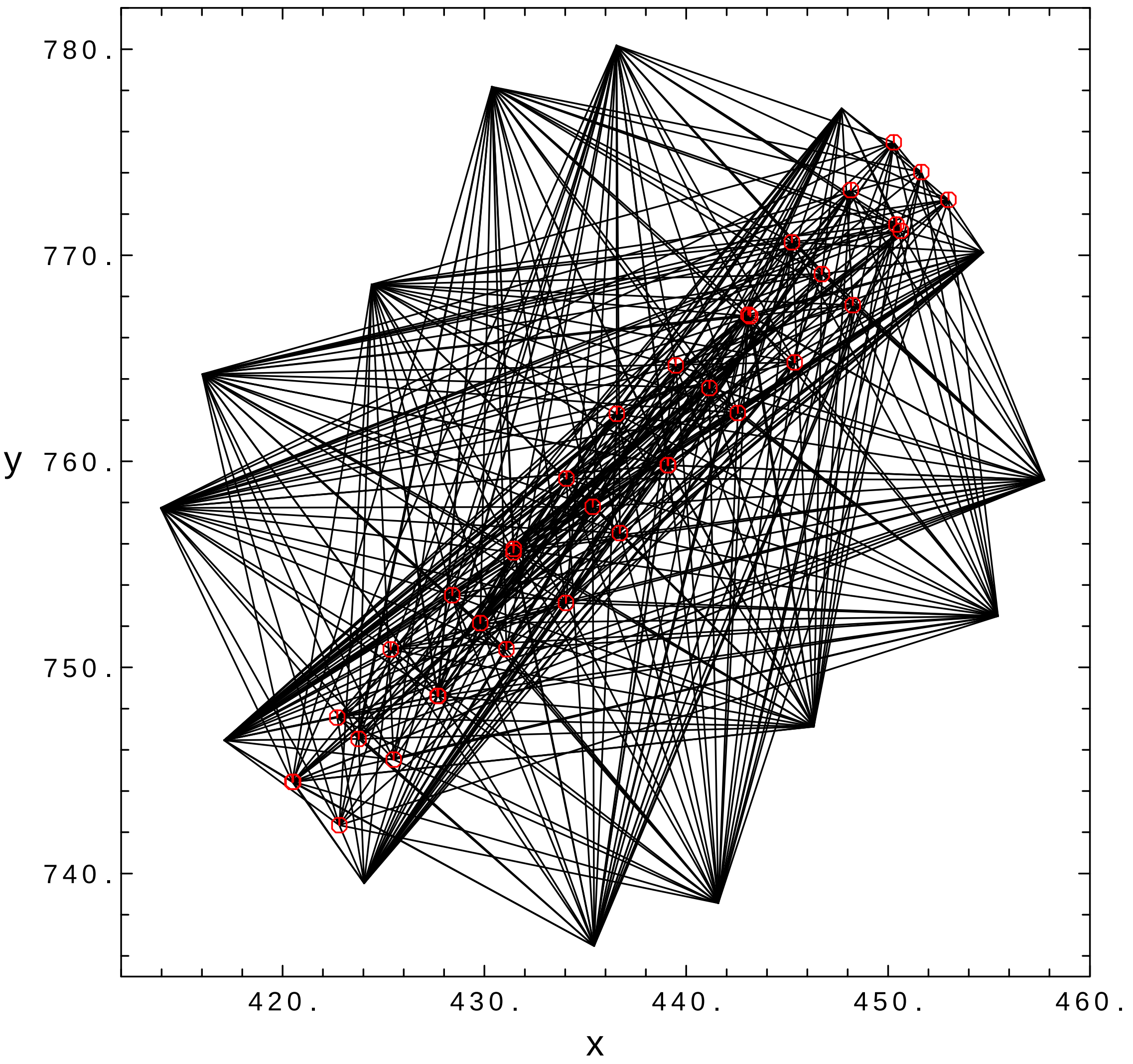

Figure 1a

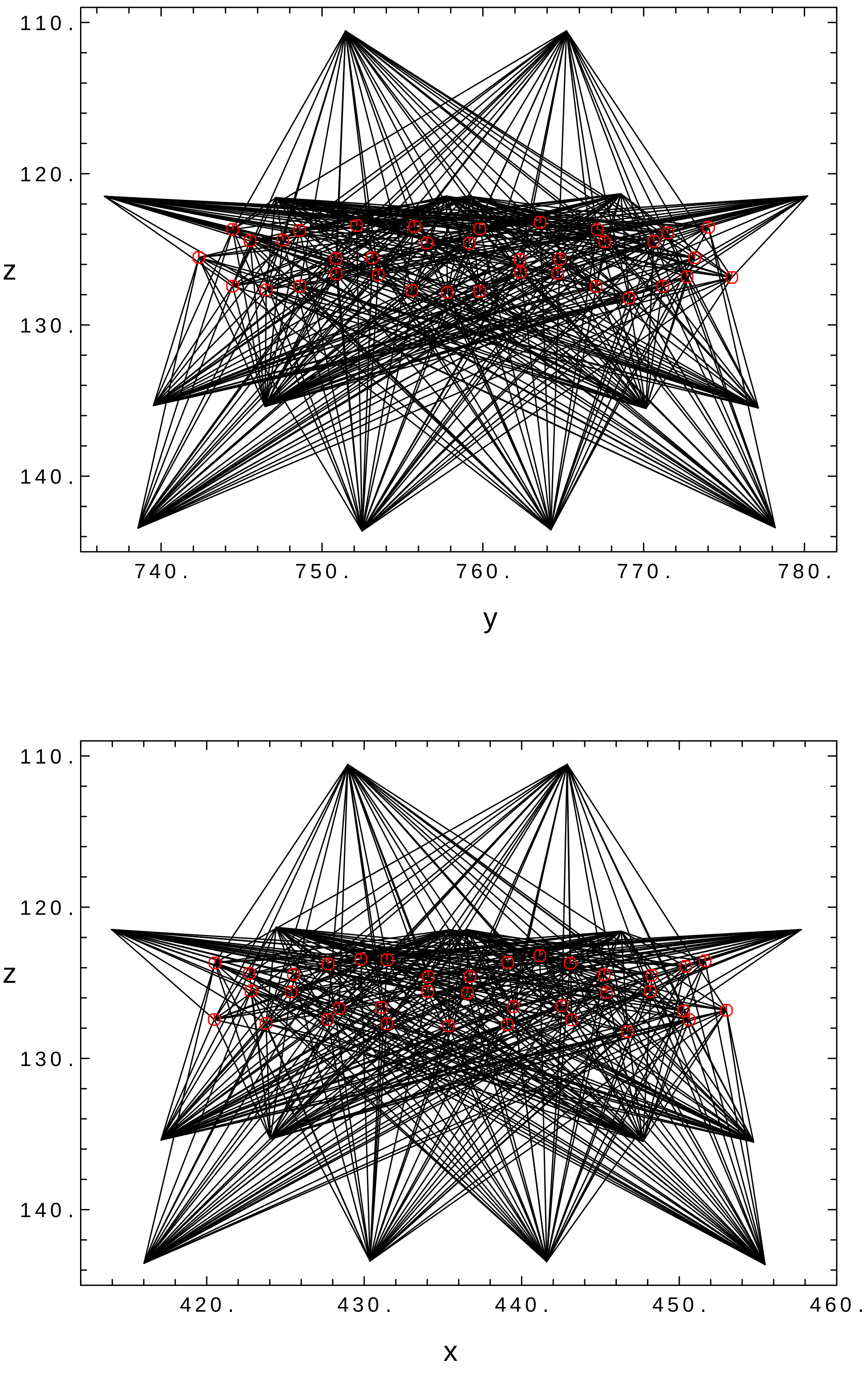
110.
120.
130.
140.
z
740.
750.
760.
770.
780.
y
110.
120.
130.
140.
z
420.
430.
440.
450.
460.
x

Figure 1b

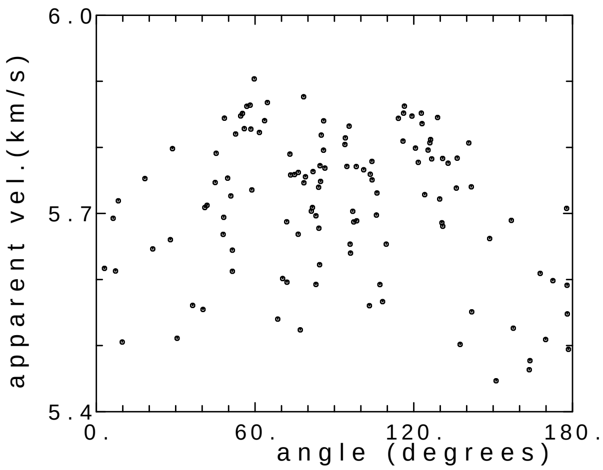

(y, z) section

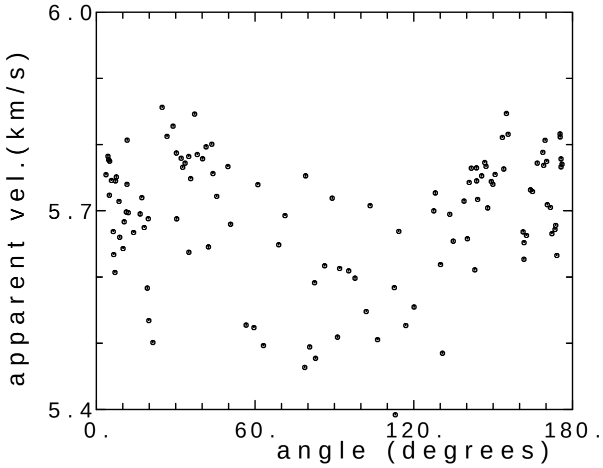

(x, z) section

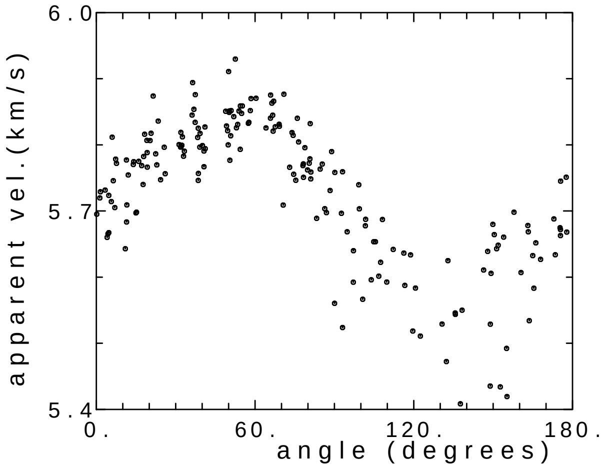

(x, y) section

Figure 2

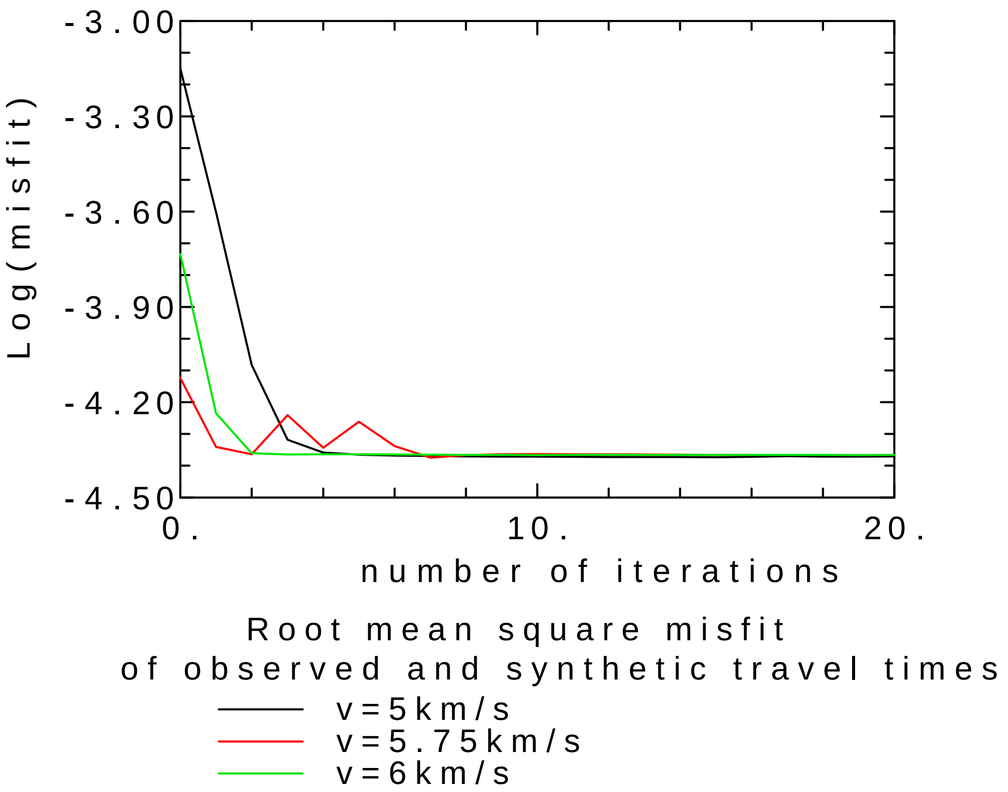
-3.00
-3.30
-3.60
-3.90
-4.20
-4.50
Log(misfit)
0.
10.
20.
number of iterations
Root mean square misfit
of observed and synthetic travel times
v=5km/s
v=5.75km/s
v=6km/s

Figure 3

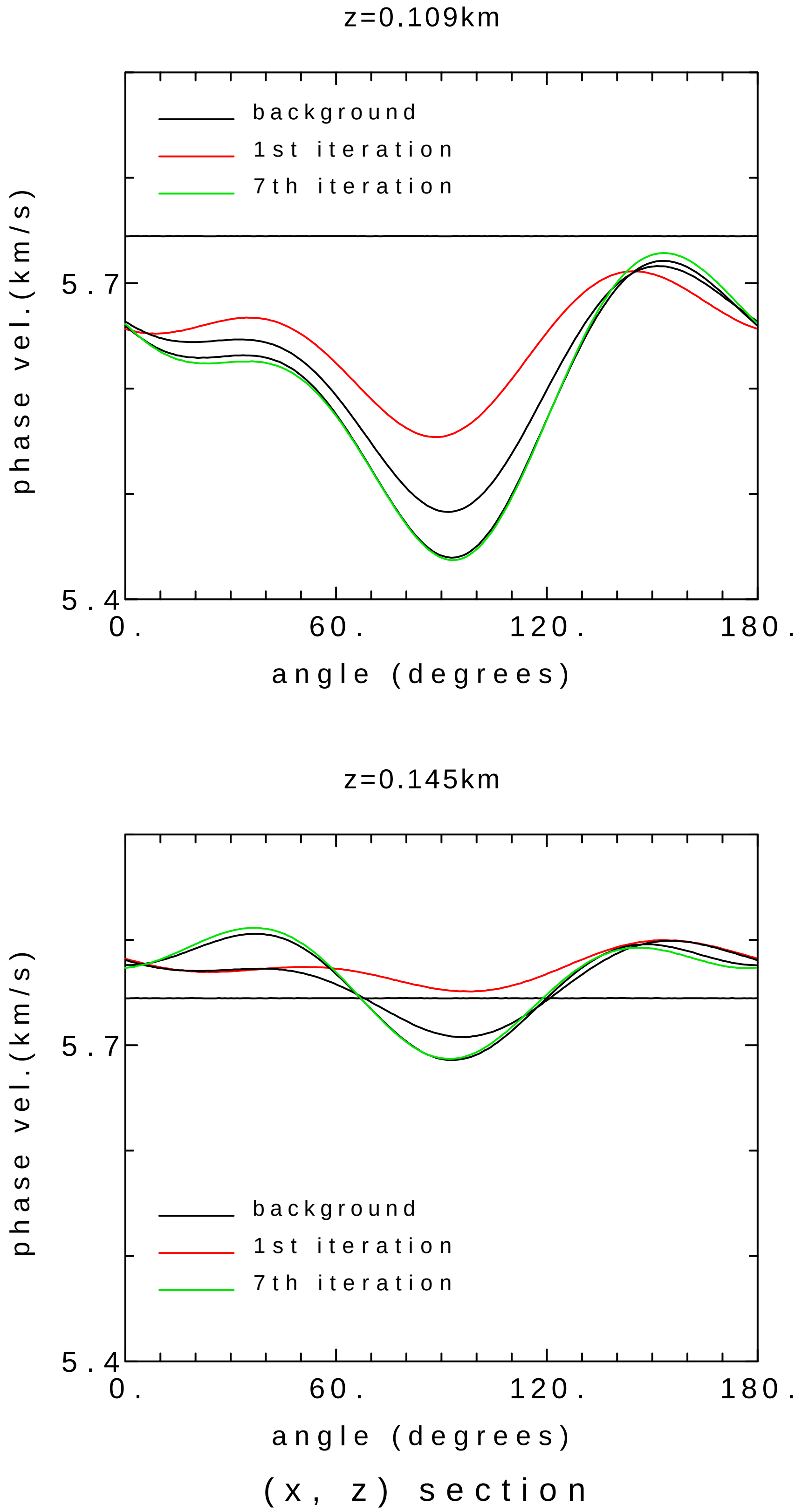
z=0.109km
background
1st iteration
7th iteration
phase vel.(km/s)
5.7
5.4
0.
60.
120.
180.
angle (degrees)
z=0.145km
background
1st iteration
7th iteration
phase vel.(km/s)
5.7
5.4
0.
60.
120.
180.
angle (degrees)
(x, z) section

Figure 4

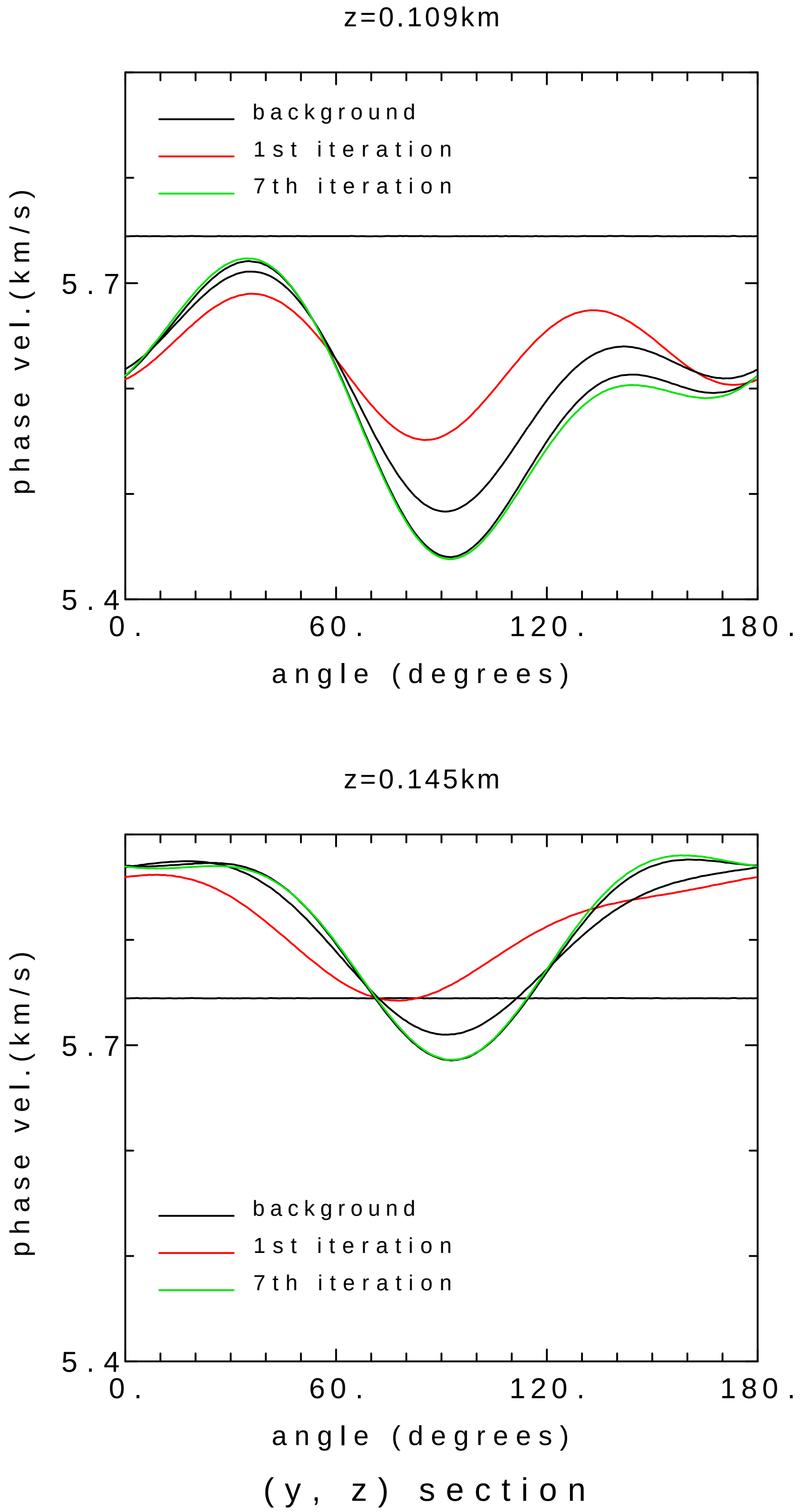
z=0.109km
background
1st iteration
7th iteration
phase vel.(km/s)
5.7
5.4
0.
60.
120.
180.
angle (degrees)
z=0.145km
background
1st iteration
7th iteration
phase vel.(km/s)
5.7
5.4
0.
60.
120.
180.
angle (degrees)
(y, z) section

Figure 5

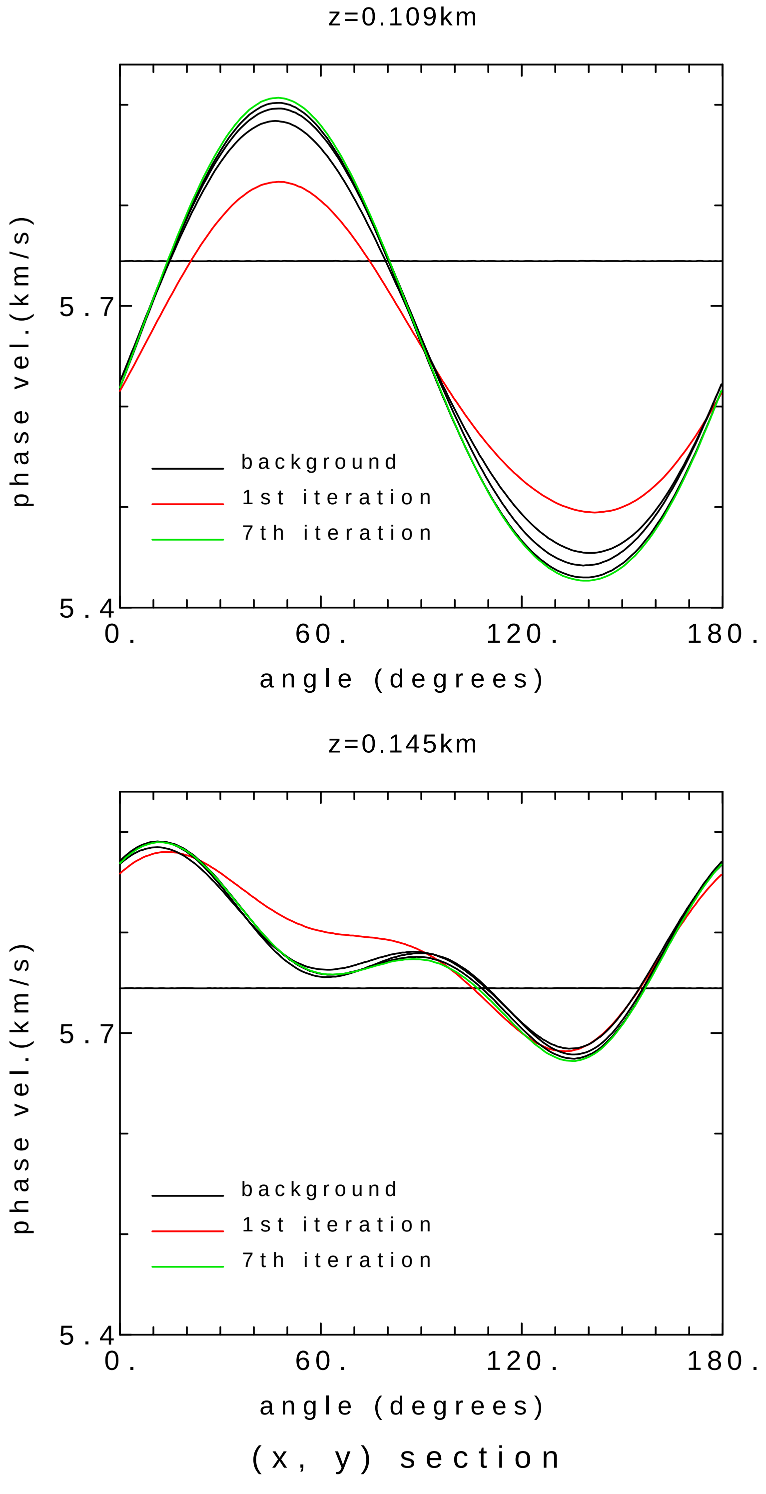
z=0.109km
phase vel.(km/s)
5.7
5.4
0.
60.
120.
180.
angle (degrees)
background
1st iteration
7th iteration
z=0.145km
phase vel.(km/s)
5.7
5.4
0.
60.
120.
180.
angle (degrees)
background
1st iteration
7th iteration
(x, y) section

Figure 6

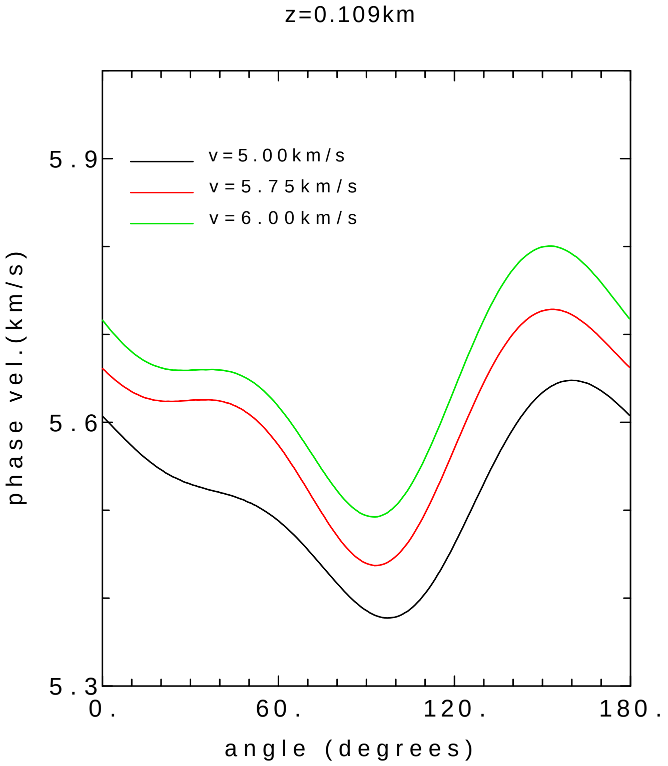
z=0.109km
v=5.00km/s
v=5.75km/s
v=6.00km/s
5.9
5.6
5.3
0.
60.
120.
180.
phase vel.(km/s)
angle (degrees)

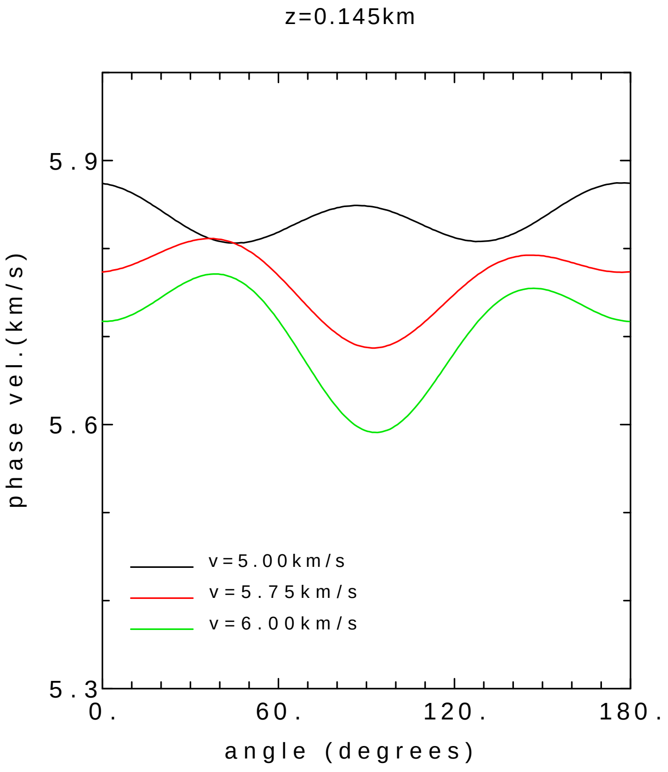
z=0.145km
v=5.00km/s
v=5.75km/s
v=6.00km/s
5.9
5.6
5.3
0.
60.
120.
180.
phase vel.(km/s)
angle (degrees)
(x, z) section

Figure 7

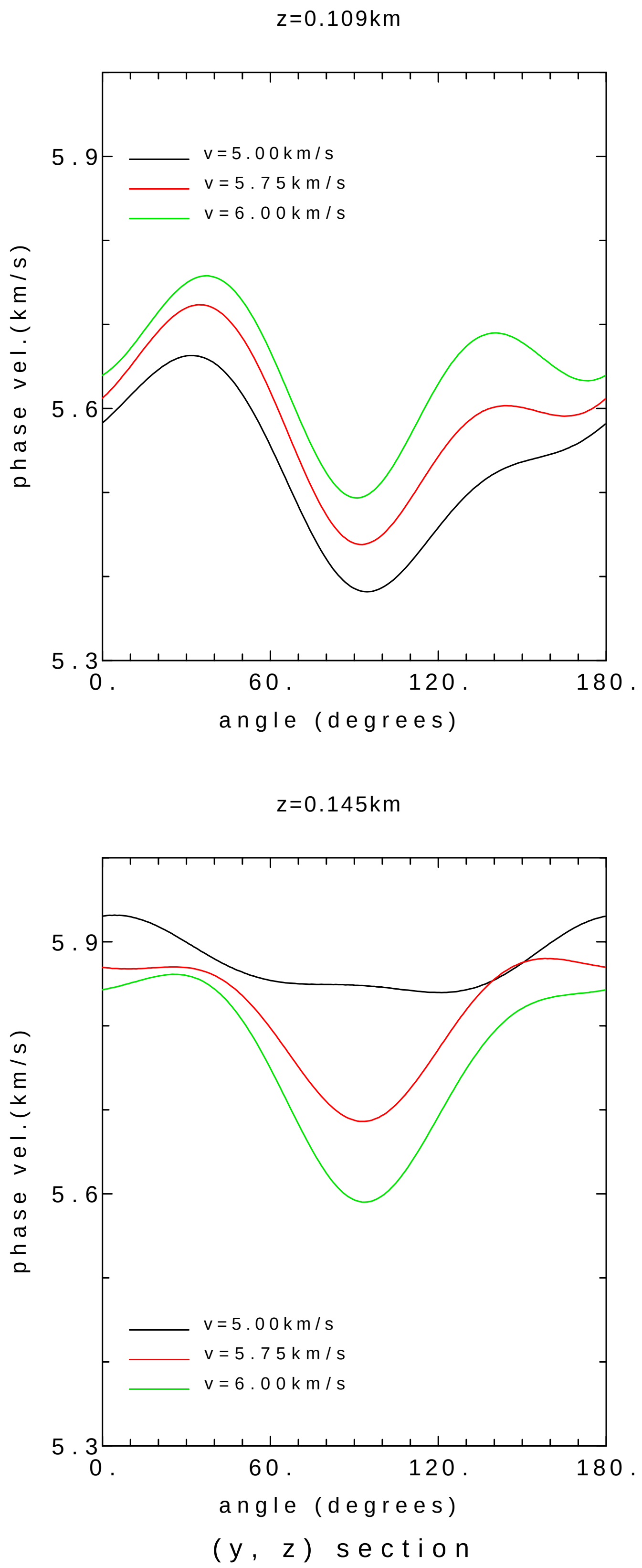
z=0.109km
v=5.00km/s
v=5.75km/s
v=6.00km/s
phase vel.(km/s)
5.9
5.6
5.3
0.
60.
120.
180.
angle (degrees)
z=0.145km
v=5.00km/s
v=5.75km/s
v=6.00km/s
phase vel.(km/s)
5.9
5.6
5.3
0.
60.
120.
180.
angle (degrees)
(y, z) section

Figure 8

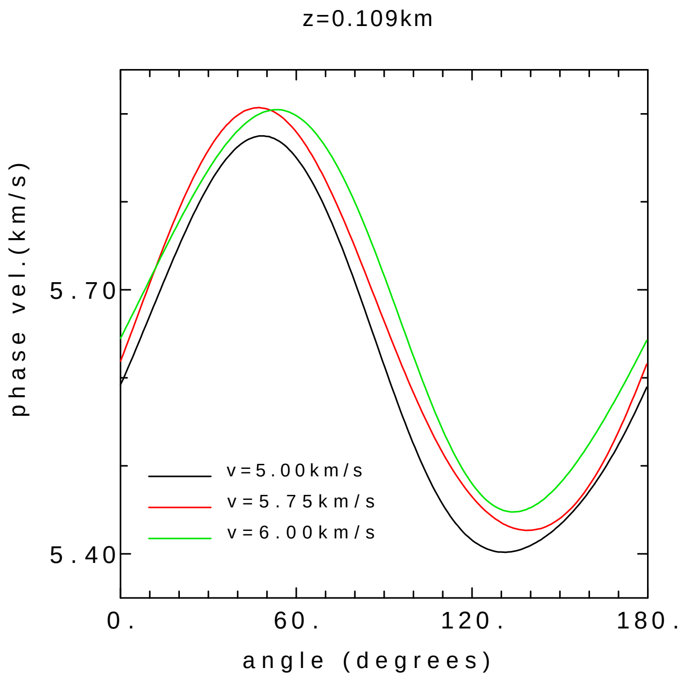
z=0.109km
phase vel.(km/s)
5.70
5.40
v=5.00km/s
v=5.75km/s
v=6.00km/s
0.
60.
120.
180.
angle (degrees)

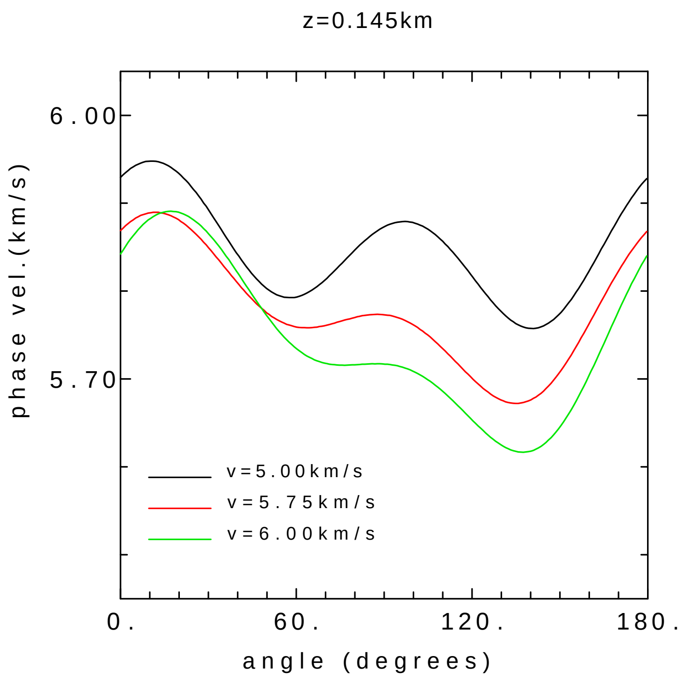
z=0.145km
phase vel.(km/s)
6.00
5.70
v=5.00km/s
v=5.75km/s
v=6.00km/s
0.
60.
120.
180.
angle (degrees)
(x, y) section

Figure 9

Top

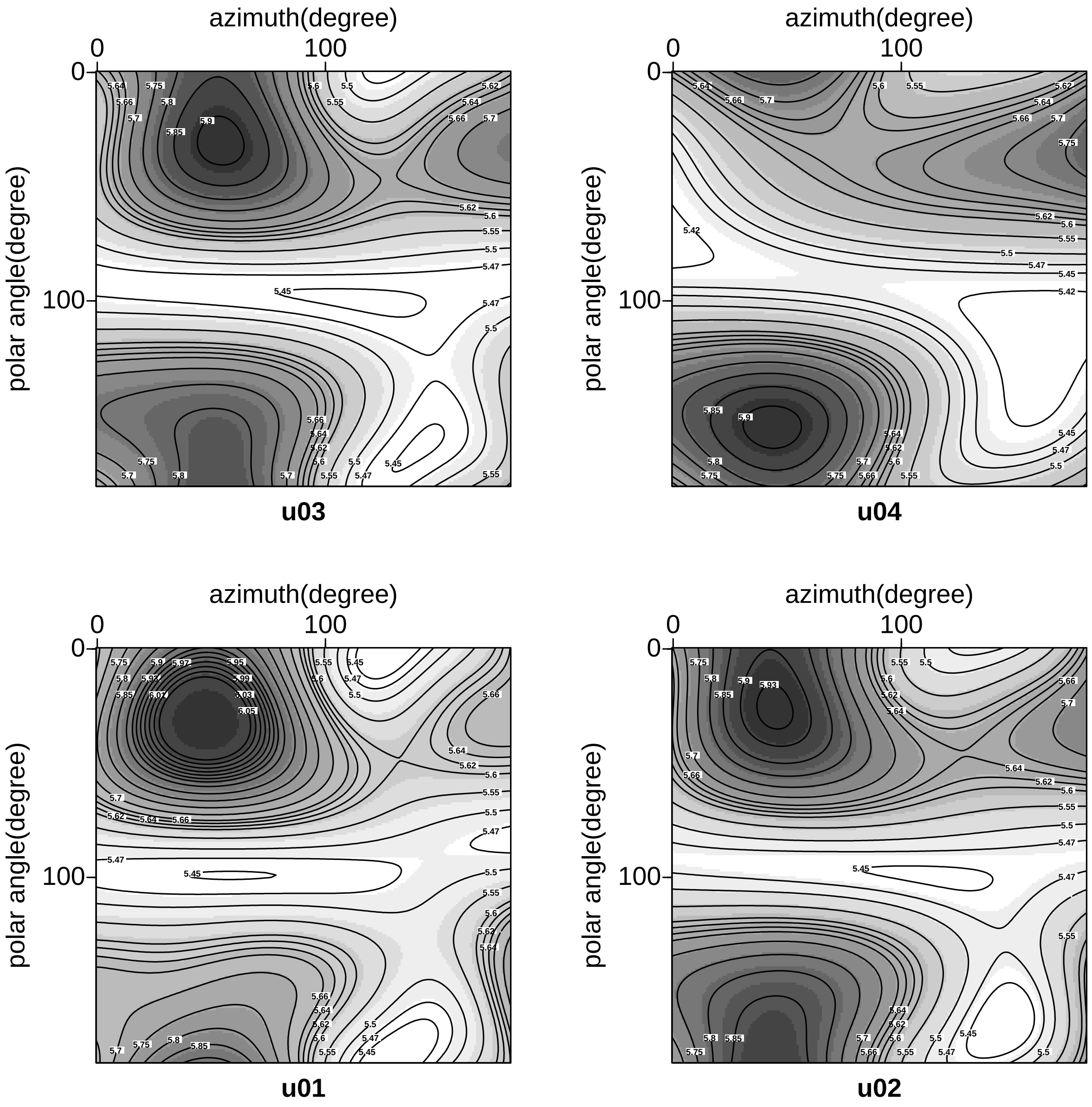

Figure 10a

Bottom

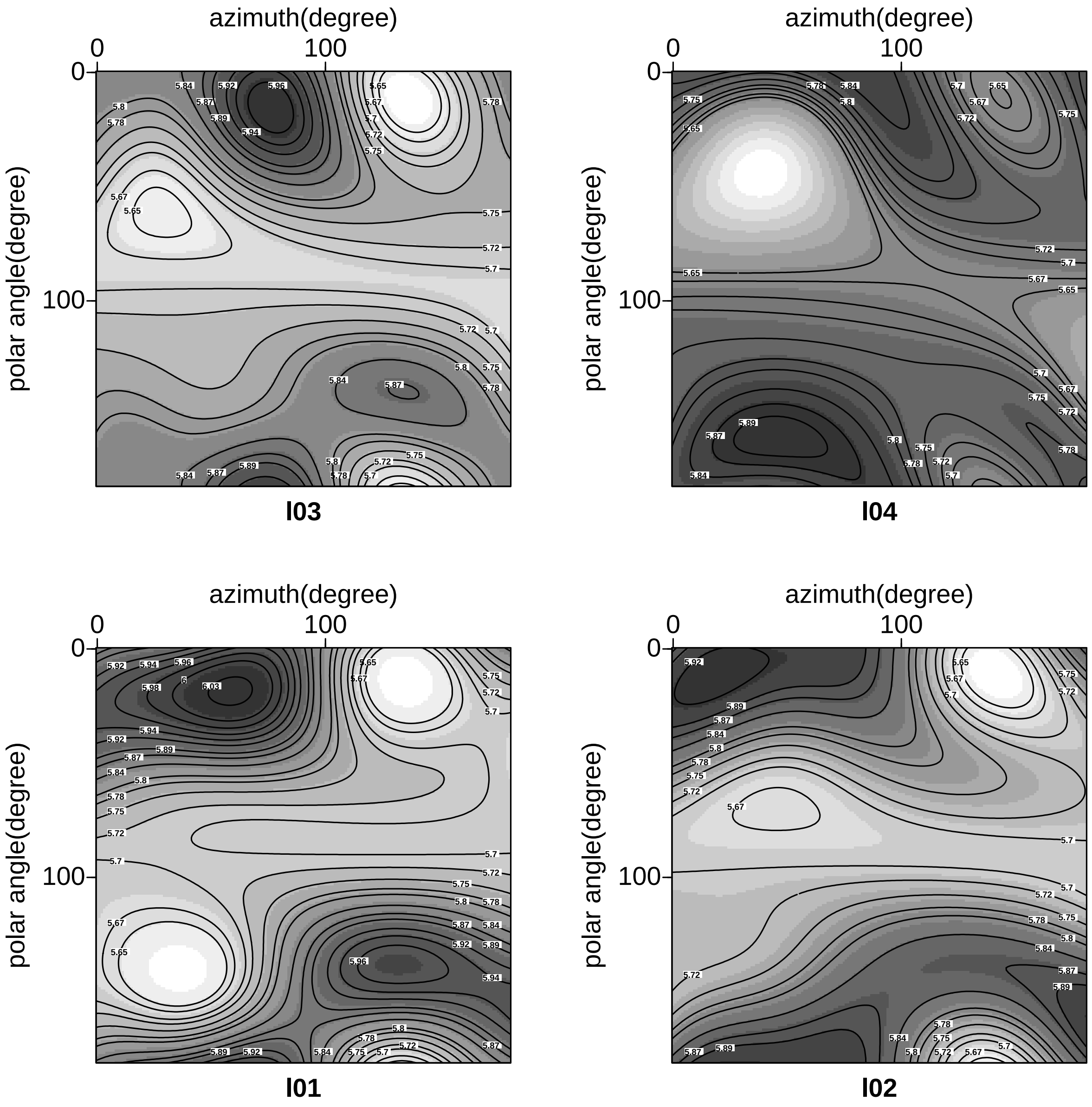

Figure 10b

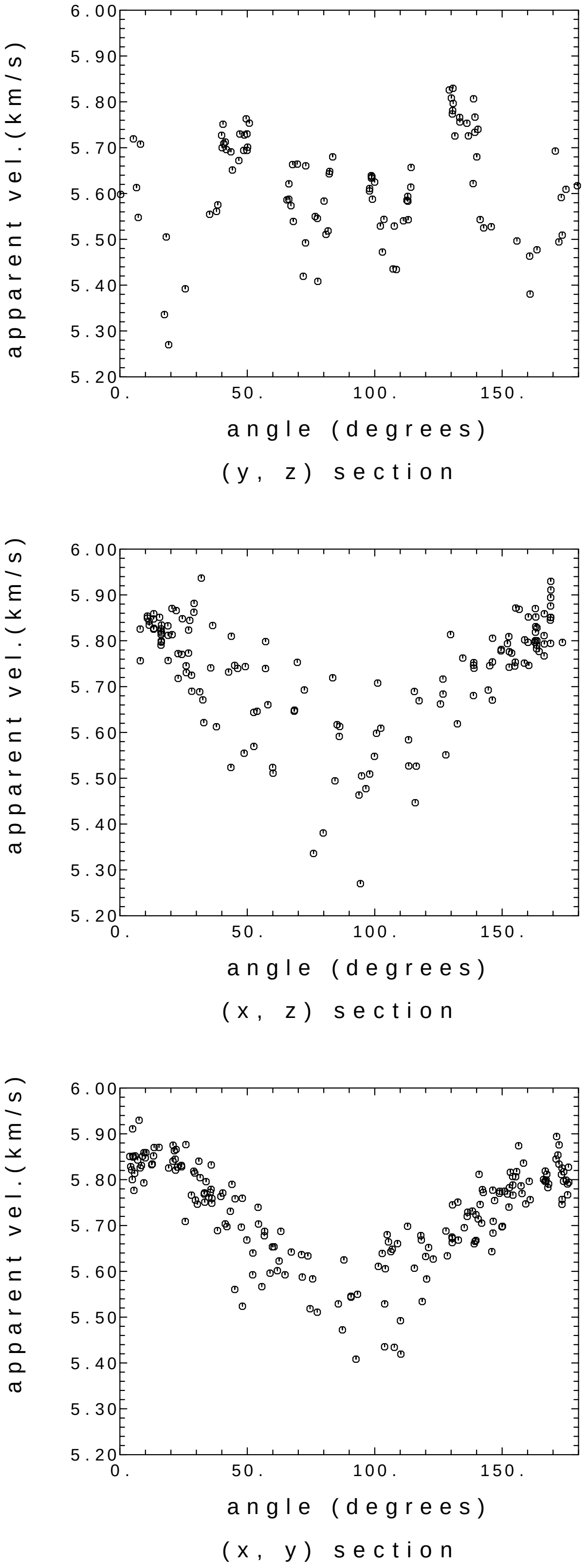
6.00
5.90
5.80
5.70
5.60
5.50
5.40
5.30
5.20
apparent vel.(km/s)
0.
50.
100.
150.
angle (degrees)
(y, z) section
(x, z) section
(x, y) section

Figure 11

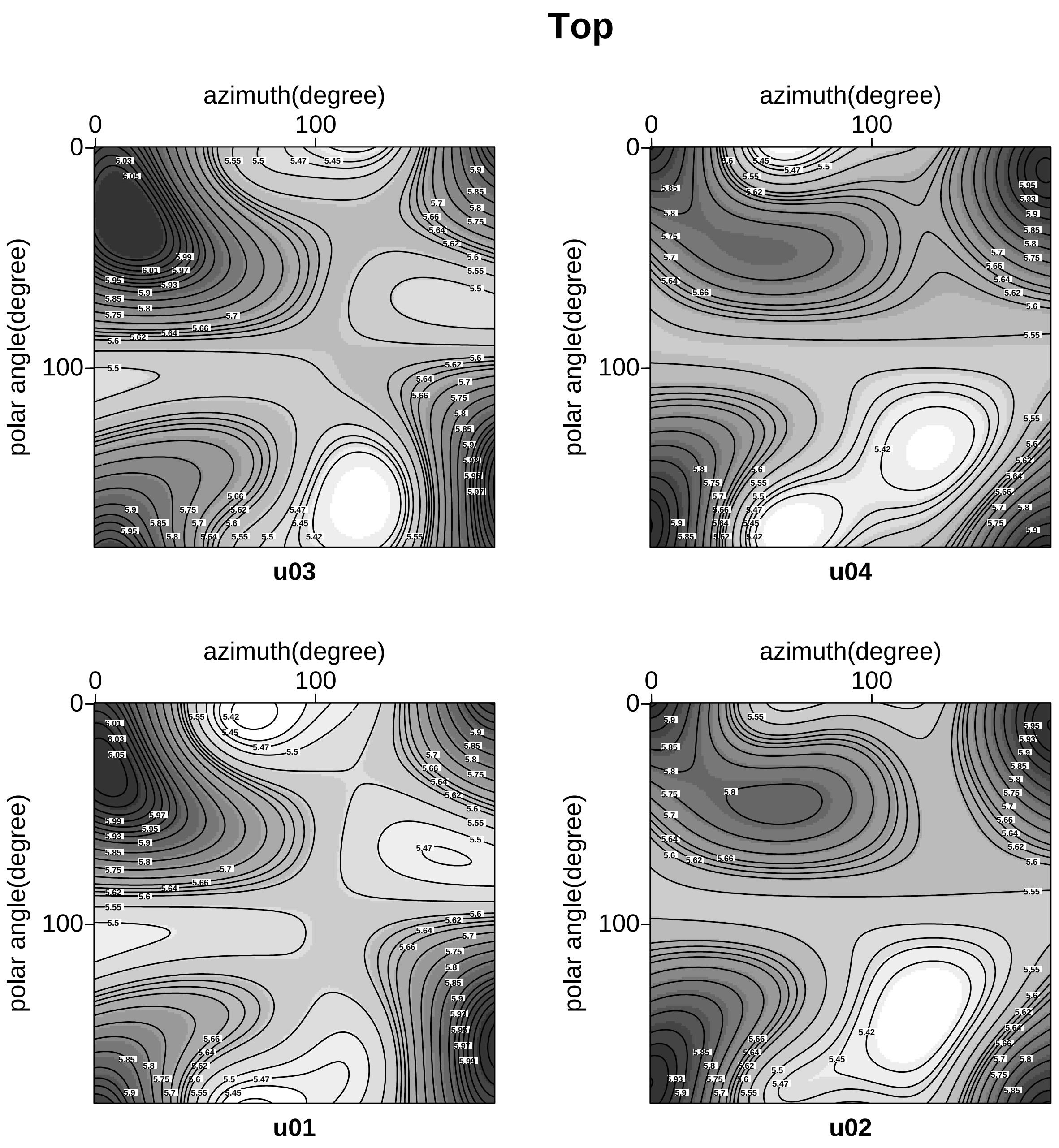
Top
azimuth(degree)
0
100
polar angle(degree)
0
100
u03
u04
u01
u02

Figure 12a

Bottom

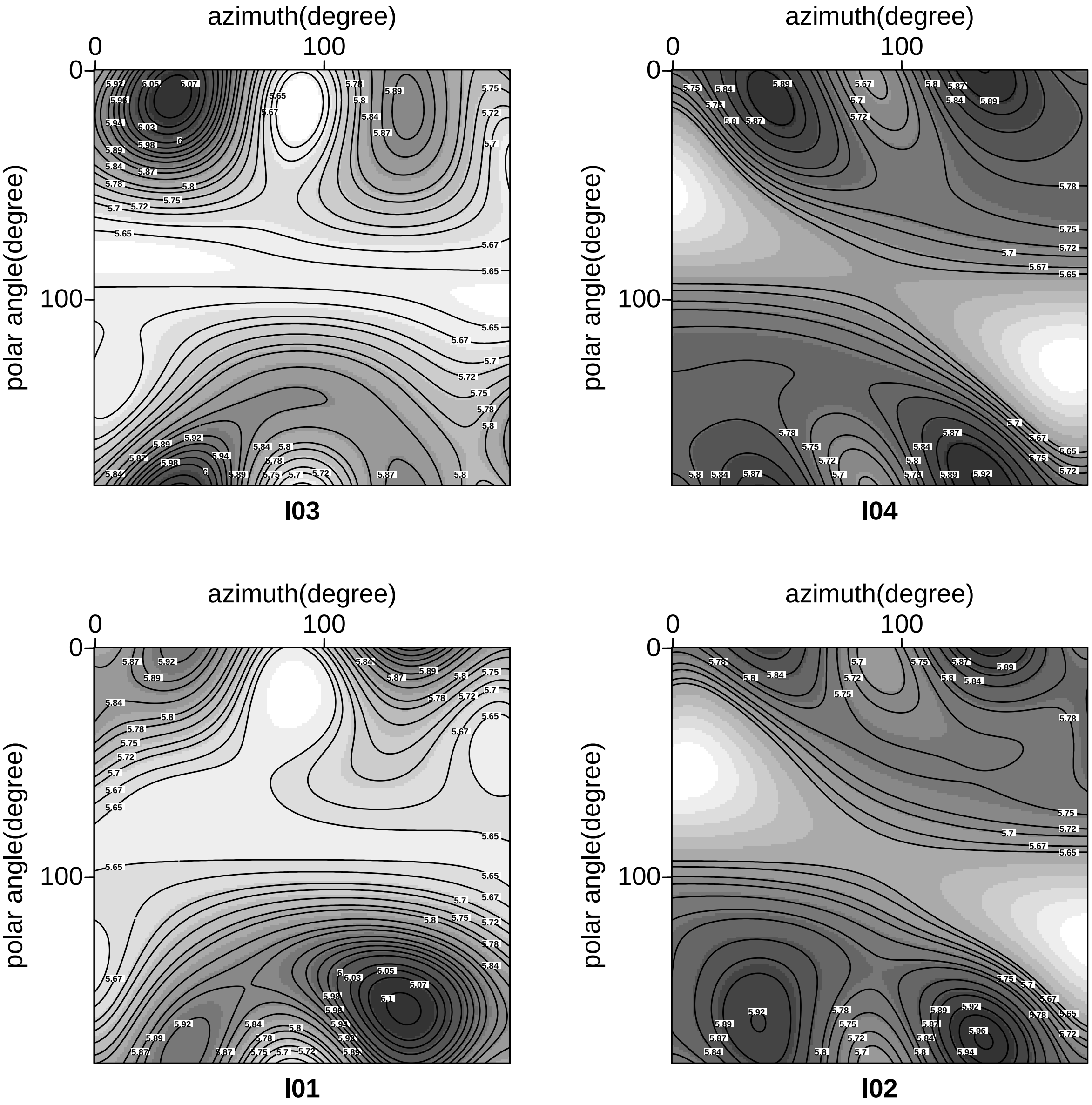

Figure 12b

Front

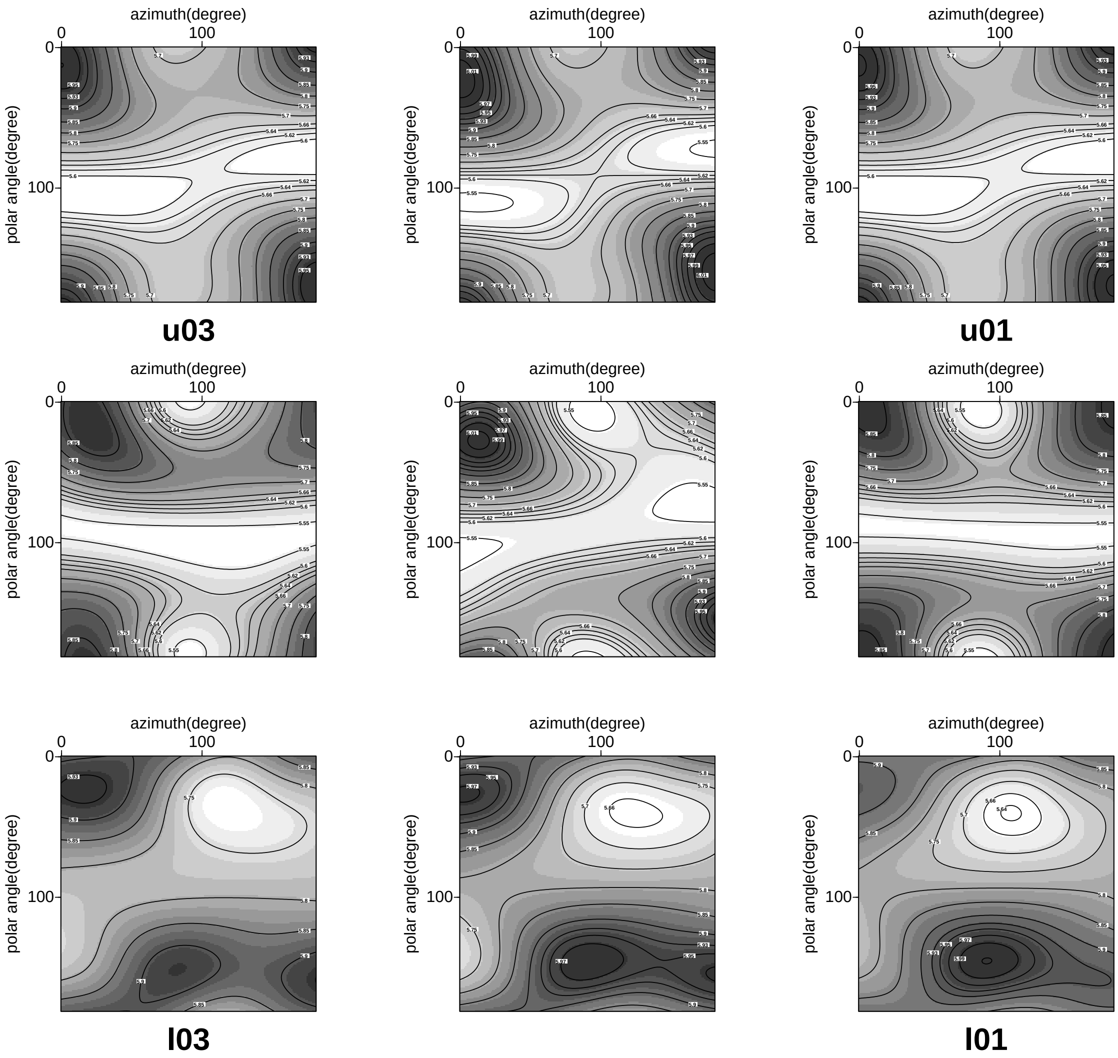

Figure 13a

Rear

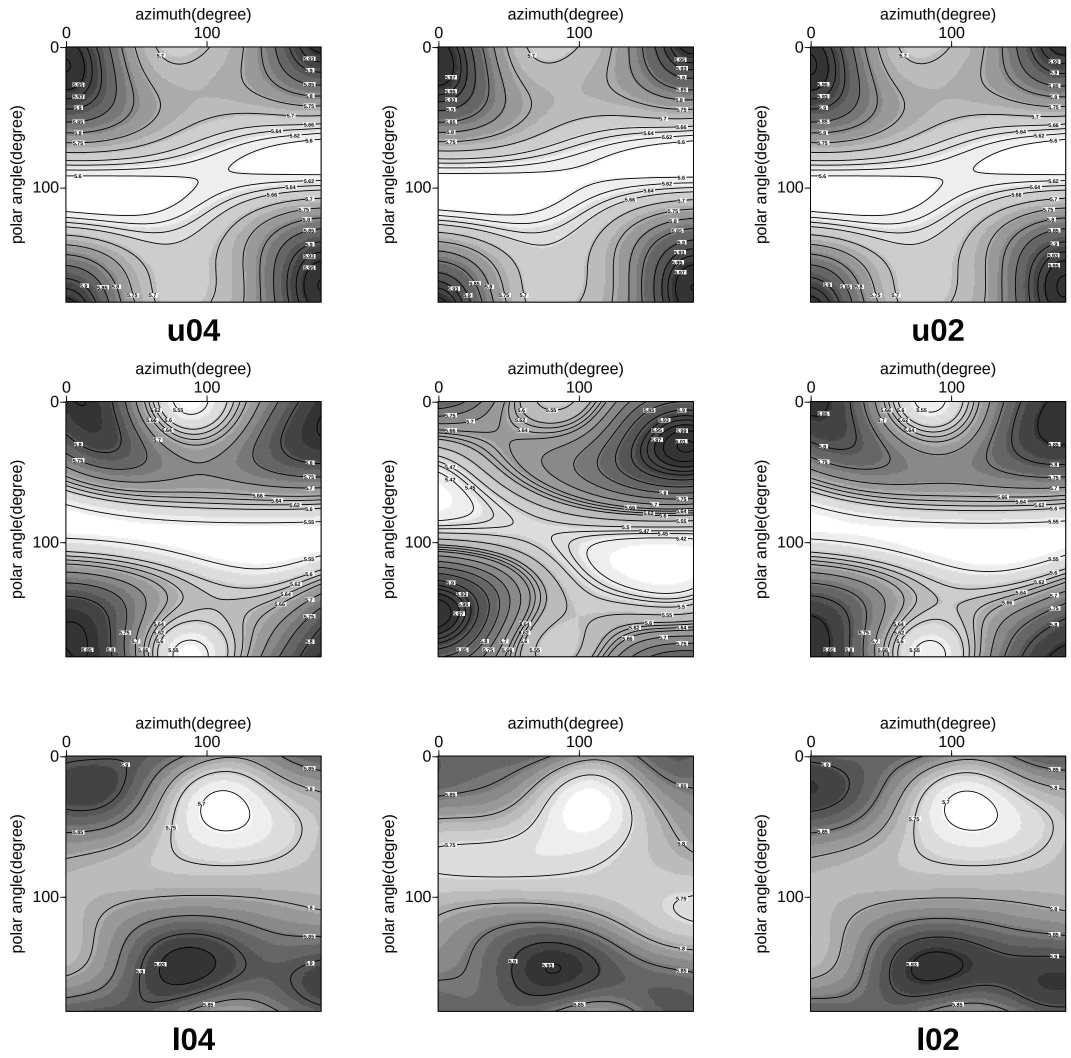

Figure 13b

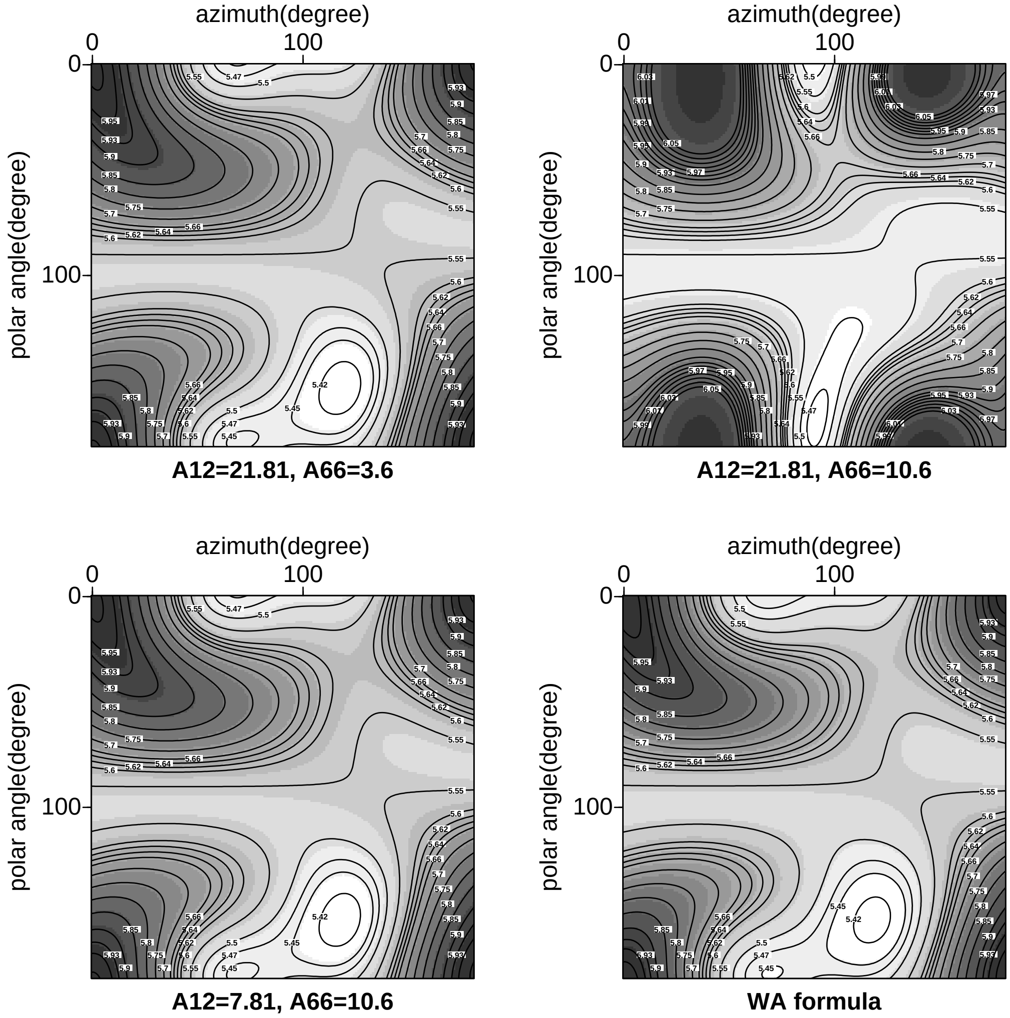

azimuth(degree)
0
100
polar angle(degree)
A12=21.81, A66=3.6
A12=21.81, A66=10.6
A12=7.81, A66=10.6
WA formula

Figure 14